AIAA 95-2314
Hypervelocity Aeroheating Measurements in Wake of Mars Mission Entry Vehicle

Brian R. Hollis, John N. Perkins
North Carolina State University
Raleigh, NC

26th AIAA Fluid Dynamics Conference

June 19-22, 1995/San Diego, CA

Hypervelocity Aeroheating Measurements in Wake of Mars Mission Entry Vehicle

Brian R. Hollis* and John N. Perkins†
Department of Mechanical and Aerospace Engineering
North Carolina State University
Raleigh, NC 27695-7921

ABSTRACT

Detailed measurements of aerodynamic heating rates in the wake of a Mars-Pathfinder configuration model have been made. Heating data were obtained in a conventional wind tunnel, the NASA LaRC 31" Mach 10 Air Tunnel, and in a high-enthalpy impulse facility, the NASA HYPULSE expansion tube, in which air and CO_2 were employed as test gases. The enthalpy levels were 0.7 MJ/kg in the Mach 10 Tunnel, 12 MJ/kg at Mach 9.8 for HYPULSE CO_2 tests and 14 MJ/kg at Mach 7.9 for HYPULSE air tests. Wake heating rates were also measured on three similar parametric configurations, and forebody heating measurements were made in order to facilitate CFD comparisons. The ratio of peak wake heating to forebody stagnation point heating in the Mach 10 Tunnel varied from 7% to 15% depending on the freestream Reynolds number. In HYPULSE, the ratio was ~5% for both air and CO_2. It was observed that an increase in the ratio of forebody corner radius to nose radius resulted in a decrease in peak wake heating, and moved the peak closer to the base of the forebody. The wake flow establishment process in HYPULSE was studied, and a method was developed to determine when the wake has become fully established.

BACKGROUND

Like the earlier Mars-Viking probe, the Mars-Pathfinder (previously known as MESUR) vehicle currently being designed by NASA[1] will be equipped with a 70° sphere-cone geometry aeroshell. In the design of planetary entry vehicles such as these, the behavior of the flow in the wake of the forebody aeroshell is an important factor in payload size, placement, and heat shielding requirements.

The object of this study was to generate a data set of wake heating measurements for use in the design of future such vehicles, and to study the wake flow establishment process in an impulse facility. Forebody heating measurements were also included in this research to aid in CFD code calibration exercises.

MODEL DESCRIPTIONS

The focus of this study was on heating measurements in the wake of a Mars-Pathfinder configuration model; however, limited parametric studies were also conducted by measuring wake heating rates generated by three similar forebody configurations. The four configurations are depicted in Figure 1, along with the model dimensions. All four configurations had an identical afterbody which was defined by that of the Mars-Pathfinder configuration. This Mars-Pathfinder configuration will be referred to hereinafter as MP-1. The MP-2 configuration was a hyperboloid with the same nose radius of curvature and base diameter as MP-1. The MP-3 and MP-4 configurations were identical to MP-1 except for their corner radii, which were double or quadruple, respectively, the corner radius of MP-1. All four configurations were equipped with identical stings.

Models of the four configurations were machined from Macor ceramic and instrumented with thin-film temperature resistance gages as described in Reference 2. Uninstrumented models were also machined from stainless steel. Each instrumented model had 37 thin-film gages located along a single ray which covered both the forebody and afterbody. Stings for the models were machined from stainless steel, and each carried a Macor insert with an additional 33 thin-film gages.

---

* Graduate Research Assistant

† Professor, Mechanical and Aerospace Engineering Dept., Associate Fellow AIAA

FACILITY DESCRIPTIONS

Aerodynamic heating tests were conducted in two hypersonic experimental facilities: the NASA Langley Research Center 31" Mach 10 Air Tunnel [3] and the NASA HYPULSE [4] (HYpervelocity imPULSE) Expansion Tube at the General Applied Sciences Laboratories. Representative flow conditions for these facilities are given in Table 1.

The LaRC 31" Mach 10 facility is a conventional low-enthalpy wind tunnel, currently operated only in blowdown mode but capable of continuous flow operation. Its high flow quality and relatively large test core (~14" dia.), combined with its high temperature driver potential make this a valuable aerothermodynamic research facility. Test times in the 31" Mach 10 Air Tunnel for this study were 3-5 seconds (longer test times are possible for aerodynamic studies) and data was sampled at a rate of 50 Hz.

HYPULSE is a 6" diameter shock-expansion tube in which steady, hypervelocity, high-enthalpy flows can be generated without the freestream test gas dissociation which occurs in a reflected shock tunnel. This combination of high enthalpy and steady, undissociated flow make HYPULSE an ideal facility for simulation of atmospheric entry conditions. The HYPULSE Expansion Tube can be operated with a number of different gases, although in this study only CO_2 and air were employed. HYPULSE test times for this study were on the order of 200-400 μsec, and the data sampling rate was 500 kHz.

DATA REDUCTION

Heating rates were computed from measured thin-film gage temperature-time histories using the classical constant substrate thermal properties, one-dimensional, semi-infinite solid method developed by Cook [5]:

$$\dot{q}(t_n) = \frac{2\beta}{\sqrt{\pi}} \sum_{i=1}^{i=n} \frac{T_i - T_{i-1}}{\sqrt{t_n - t_i} + \sqrt{t_n - t_{i-1}}} \qquad (1)$$

Equation 1 is referred to as the direct method; heating rates were also computed using the indirect method developed by Kendall et al [6,7]

$$Q(t_n) = \frac{\beta}{\sqrt{\pi}} \sum_{i=1}^{n} \frac{T_i + T_{i-1}}{\sqrt{t_n - t_i} + \sqrt{t_n - t_{i-1}}} \Delta t \qquad (2a)$$

$$\dot{q}(t_n) = \frac{dQ_n}{dt} = \frac{-2Q_{i-8} - Q_{i-4} + Q_{i+4} + 2Q_{i+8}}{40\Delta t} \qquad (2b)$$

Over a given time interval, both the direct and indirect methods yield nearly similar time-averaged heating rates, however the instantaneous heat transfer rates are generally not identical. This is because the temperature difference term in the numerator of (1) tends to accentuate fluctuations in $\dot{q}$, whereas the temperature sum in the numerator of (2a) and the wide differencing stencil in (2b) tend to smooth fluctuations. These features are illustrated in Figure 2, where the heating time histories of the stagnation point gage on the MP-1 model as calculated by the two methods for a test in the 31" Mach 10 Tunnel are shown.

Use of the indirect method was preferred in this research because it tended to present a clearer large scale picture of the heat transfer time history, especially in regards to the wake flow establishment process. It should be noted however, that the direct method would be more applicable in situations such as turbulent flows in which the small scale behavior of $\dot{q}$ was of interest.

Although the assumption is made in the development of both methods that the substrate material properties do not vary with temperature, Macor does in fact exhibit a non-trivial dependence on temperature. To account for this, an empirical correction factor, λ, for the thermal product, β, was derived for Macor in a manner similar to that discussed in Reference 2. The corrected heat transfer rates are given by:

$$\dot{q}_{var} = \dot{q}_{const}(1 + \lambda \Delta T) \qquad (3)$$

The validity of this empirical correction was confirmed by comparison with results obtained from an implicit, one-dimensional finite-difference data reduction scheme. The temperature dependence of the bulk material properties (thermal conductivity and thermal diffusivity) was directly accounted for in this scheme. Agreement between the finite-difference results and the results from the empirically corrected direct or indirect method results was excellent (~1-2 % error).

EXPERIMENTAL RESULTS

All four configurations were tested extensively in the 31" Mach 10 Air Tunnel. A total of 37 runs were made at nominal unit Reynolds numbers of 0.5×10^6, 1.0×10^6, and 2.0×10^6 per foot. The total enthalpy was 0.7 MJ/kg above the ambient enthalpy for these tests. The configurations were tested at angles-of-attack of 0°, -4°, -8°, and –20°. MP-1 was also tested at angle-of-attack with roll angles from 0° to 180° in order to obtain a three-dimensional picture of the heating distribution from the single ray of gages.

All configurations were also tested in the HYPULSE Expansion Tube. The Reynolds numbers were 0.2×10^6/ft for both air and CO_2, while the relative enthalpy level was 12 MJ/kg in CO_2 and 14 MJ/kg in air. The MP-1 and MP-2 configurations were tested at $\alpha = 0^\circ$ in both air and CO_2. The MP-3 and MP-4 configurations were tested in CO_2 at $\alpha = 0^\circ$. The MP–1 and MP-2 configurations were also tested in CO_2 and air at $\alpha = -4^\circ$.

The instrumented MACOR forebodies models were expended during each test in HYPULSE; therefore, the uninstrumented stainless steel models were used with the instrumented stings in order to gather additional wake flow data. A total of 26 runs were carried out in HYPULSE: 20 with instrumented forebodies and 6 with uninstrumented forebodies.

31" Mach 10 Air Tunnel Data

Space limitations preclude presentation of the entire Mach 10 Air data set in this paper; the data set will be fully detailed in later works. A representative sample is presented in Figures 3 to 7. Excellent repeatability was observed for all tests. Note that in all plots, the distance S/R_b is measured from the forebody stagnation point, while L/R_b is the distance along the sting measured from the base of the model, and both are normalized by the model base radius.

Forebody and wake heating rates for all configurations at Re = 1.0×10^6/ft and $\alpha = 0^\circ$ are shown in Figure 3. Configuration effects were very slight on the forebody except for the lower stagnation point heating of MP-2. In the wake, the heating rates for MP-3 and MP-4 were slightly lower than MP-1 and MP-2. Forebody and wake heating rates for all configurations at $\alpha = -20^\circ$ are shown in Figure 4.

Reynolds number effects on MP-1 are shown in Figure 5, where the heating rates are normalized by the stagnation point values. Although there were no Reynolds number effects on the forebody, a significant increase in wake heating with Reynolds number was observed. The heating rates of the other configurations (not shown) behaved similarly.

Heating rates for MP-1 at 0°, -4°, -12° and -20° angles-of-attack are presented in Figure 6. Heating distributions at $\alpha = -20^\circ$ with the ray of thin film gages at different roll angles are shown in Figure 7.

HYPULSE Expansion Tube data

Forebody heating results in from HYPULSE are presented in Figures 8-9. Allowing for small run-to-run variations in flow conditions (less than 5%) the CO_2 results for forebody and wake were both very repeatable. The air results were also good, though were somewhat less repeatable than those for CO_2. This was due mainly to flow conditions, which varied by 5-10% from run to run. It was also observed that the significantly higher temperatures and velocities produced in the air tests had an adverse effect on the performance of the forebody thin-film gages.

Figure 8 shows the forebody heating distributions for the four configurations in CO_2. While the stagnation region heating rates for the three sphere-cone configurations (MP-1,3,4) were nearly identical, the MP-3 and MP-4 configurations exhibited slightly higher heating along the conical portions of the forebodies. This effect appears to have been caused by the difference in the sonic line locations (due to the larger corner radii) on these configurations. Also note that although the blunter stagnation region of the MP-2 hyperboloid led to a lower stagnation point heating, the distribution asymptotically approaches that of MP-1 along the body, just as the hyperboloid geometry approaches that of the sphere-cone. Figure 9 shows the forebody heating distributions for MP-1 and MP-2 in air. Although the individual thin-film gages show more scatter in air, the relationship between the two distributions was similar to that observed in CO_2 except for the presence of a local heating peak at the corner.

Before discussing the wake flow heating data from HYPULSE, the subject of wake flow establishment must first be addressed. The establishment process is important because the time required for a wake flow to become fully established, while negligible in relation to test times in a conventional facility, can represent a significant portion of the available test time in an impulse facility. During this establishment process, wake heating distributions vary rapidly over a wide range of values before a steady, established distribution is reached. In order to determine correct wake heating values, the measured time-histories of the heat transfer rates must be carefully studied, and their behavior must be related to both the wake establishment process and the operating characteristics of the facility.

In HYPULSE, the duration of a test was dictated by the length of time between the arrival of the incident shock wave and the arrival of the expansion fan. This test window between these two points was determined by examination of wall pressure data (model size prevented use of a pitot probe) recorded at the mouth of the expansion tube. A criteria of +/- 5% maximum variation in the wall pressure was used to determine the size of the test window. On average, the

test window for CO_2 was found to be approximately 150 μsec, while that for air was approximately 100 μsec. These times were somewhat less than generally quoted for HYPULSE, but it was observed that the wake was extremely sensitive to freestream variations, and thus these more restrictive maximum test times were used. In fact, it should be noted that although the end of this window was considered to be the maximum time at which valid data could be taken due to the uncertainty in flow conditions, in some cases the heating distributions appeared to remain constant for up to 50 μsec past the end of the window.

A rigorous analysis was required to characterize the wake establishment process. In the past, flow establishment has been determined by the study of pressure or heating time history data of individual gages. The flow at a given point was said to be "established" when the measured values reached some percentage (~95%) of their mean values. However, because the mean values could not be known a priori, this approach could be subject to interpretation. Furthermore, the established values at different locations could be reached at different times, which made this analysis more complicated. For these reasons, it was decided that an integrated process for determining when the entire wake flow became established was required.

Initially, plots of heating rate vs. position were generated at each discrete time during the test at which data was recorded. A computer slide show "movie" of these distributions was then generated using commercially available software. These motion pictures provided a graphical illustration of the establishment process, and the point at which the heating distributions stabilized throughout the wake could usually be clearly identified. An analog of one such movie is presented in Figure 10, in which heating distributions at several times are overlaid on a single plot. In the period immediately after the incident shock arrival, the heating rates fluctuated rapidly as the outer inviscid core of the wake was established. The heating rate distribution then began to gradually approach a steady-state value as the recirculation region immediately behind the base grew. The distribution then remained at the established steady-state until the expansion fan arrived and the test period ended.

Although a valuable analysis tool, the motion picture approach was without theoretical foundation, as the decision on when the flow was established could still be somewhat arbitrary. Also, as Figure 10 illustrates, the presentation of a movie in a hard copy format is problematical at best. A criteria for wake flow establishment with more physical/mathematical foundations was obtained through the use of a normalized heat transfer "residual" defined by:

$$\sigma(t) = \frac{\Delta \dot{q}}{\dot{q}} \tag{3}$$

where

$$\Delta \dot{q} = \frac{M\dot{q}}{Mt}\Delta t$$

From the individual residual-time histories for each gage an overall root-mean-square variation for the entire wake region was computed by:

$$RMS(\sigma) = \sqrt{\frac{1}{n}(\sigma_1^2+\sigma_2^2 + \ ... \ + \sigma_n^2)} \tag{4}$$

Although RMS calculations are normally associated with the study of high frequency behavior induced by noise or turbulence, the lower frequency flow processes associated with wake establishment were captured by computing a heat flux time derivative based on the indirect method of Equations 2a-2b. It also should be noted that because the HYPULSE driving temperatures were much greater than the measured wall temperatures, the established heating rates could be expected to remain constant, and thus there were no wall temperature effects on the RMS calculations.

In general, it was observed that the wake heating RMS was initially extremely high due to the arrival of the incident shock and the forebody flow establishment process (which required on the order of 50 μsec) and then tended toward zero as the wake flow established. This behavior can be seen in Figure 11 in which the RMS time history of the same test depicted in Figure 10 is presented. The incident shock arrival, the establishment of the inviscid and recirculation regions of the wake, and the arrival of the expansion fan can all be seen in this RMS time history. An establishment criteria of ~ 0.02 for the wake flow RMS was set. This value was in part determined by observation of the RMS values at the times at which the motion pictures showed that the heating distributions were constant.

Based on the times determined from the RMS approach, the non-dimensional establishment parameter was computed:

$$\tau = \frac{U_4 t_{est}}{y_{ref}} \tag{5}$$

where in this case the reference dimension, y, was taken to be the difference between the model base radius and the sting radius. The establishment parameter values fell between 45 and 75 for both the air and CO_2 tests, which was consistent with previous results[8], and fell within the available HYPULSE test times. The average value in air was 67 and in CO_2 was 56. Establishment parameter values were generally slightly lower in tests

where the models were at a -4˚ angle-of-attack.

The wake heating rates were averaged over the established times determined from the RMS values. Results are presented in Figures 12-14. In Figure 12, heating distributions for each of the four configurations in CO_2 are shown. MP-1 and MP-2 wake distributions were as expected essentially identical, as were the forebody distributions away from the stagnation point. The MP-3 and MP-4 distributions show that increasing the corner radius decreases the peak wake heating value and moves the peak in toward the model base. Based on these values, the ratios of peak wake heating to measured stagnation point heating were ~5% for MP-1, ~6% for MP-2, ~4% for MP-3, and ~3% for MP-4.

Angle-of-attack test results in CO_2 are given in Figure 13. At α = -4˚, the peak heating was only slightly higher, although the peak location was much closer to the base, while the peak was considerably higher in the single α = -8˚ test.

Angle-of-attack and configuration effects for the air tests are shown in Figure 14. The MP-1 and MP-2 configuration distributions were again in close agreement. However in air, the change in peak heating magnitude and location with α was greater. The wake to stagnation point ratios in air at α = 0˚ were again ~5% for MP-1 and ~6% for MP-2.

Comparison of Mach 10 and HYPULSE data

Normalized heating distributions for the MP-1 Mars-Pathfinder configuration tests in HYPULSE and the 31" Mach 10 Tunnel are given in Figures 15-16. Normalized forebody distributions in air were nearly identical at the three Mach 10 Reynolds numbers and in the HYPULSE tests, but there was a noticeable difference between the air and CO_2 results. In the wake, the normalized distributions differed considerably. While the decrease in peak heating at the HYPULSE Reynolds number was roughly consistent with the trend observed in the 31" Mach 10 Tunnel, the location of the peak was moved closer to the body instead of further downstream as the Mach 10 data would suggest, which indicates that chemistry at the HYPULSE flow conditions had a significant effect on the wake structure. Data from the other configurations (not shown) indicated similar behavior.

SUMMARY

A Mars-Pathfinder entry vehicle model and three similar configurations were tested in a conventional wind tunnel and in a high-enthalpy, hypervelocity impulse facility.

Detailed aerodynamic heating measurements were made on instrumented stings in the wake of the models and on the model forebodies. Forebody heating distributions for all four configurations were similar; however the hyperboloid configuration had a lower stagnation point heating rate, while the larger corner radii sphere-cone configurations had slightly higher heating along their conical sections. Wake heating rates were considerably lower than forebody heating rates. In the 31" Mach 10 Air Tunnel, the peak wake heating to stagnation point heating ratio varied with Reynolds number from 7% to 15% at a constant relative enthalpy level of 0.7 MJ/kg. In the HYPULSE Expansion Tube, the ratio was 5% in air with a 14 MJ/kg enthalpy level and was also 5% in CO_2 with a 12 MJ/kg enthalpy level.

The wake flow establishment process was studied, and a method to characterize the establishment based on the RMS of the heating rate residual was developed. HYPULSE tests times were found to be sufficient for flow establishment. The non-dimensional establishment time varied from 45-75, with the establishment in CO_2 taking slightly less time than in air.

ACKNOWLEDGEMENTS

This work was supported in part by the North Carolina State University Mars Mission Research Center under grants NAGW-1331 and NAG-1-1663. Funding for model construction and experimental testing was provided by the Aerothermodynamics Branch, NASA Langley Research Center.

REFERENCES

[1] Hubbard, G.S., et al, “A Mars Environmental Survey (MESUR) -- Feasibility of a Low Cost Global Approach,” IAF Paper No. 91-432, Oct. 1991.

[2] Miller, C.G., "Comparison of Thin-Film Resistance Heat-Transfer Gages With Thin-Skin Transient Calorimeter Gages in Conventional Wind Tunnels," NASA TM 83197, Dec. 1981.

[3] Miller, C.G., "Langley Hypersonic Aerodynamic/Aerothermodynamic Testing Capabilities - Present and Future," AIAA Paper 90-1376, 1990.

[4] Tamago, J., et al , “Hypervelocity Real Gas Capabilities of GASL’s Expansion Tube

(HYPULSE) Facility," AIAA Paper 90-1390, June 1990.

[5] Cook, William J., "Unsteady Heat Transfer to A Semi-Infinite Solid With Arbitrary Surface Temperature History and Variable Thermal Properties," IOWA State University Technical Report ISU-ERI-AMES-675000, Feb. 1970.

[6] Kendall, D.N., Dixon, W. Paul, and Schulte, Edward H., "Semiconductor Surface Thermocouples for Determining Heat-Transfer Rates," IEEE Transactions on Aerospace and Electronic Systems, Vol. AES-3, No. 4, July 1967, pp.596-603.

[7] Hedlund E.R., et al, "Heat Transfer Testing in the NSWC Hypervelocity Wind Tunnel Using Co-axial Surface Thermocouples," NSWC MP 80-151, March 1980.

[8] Holden, M.S., "Establishment Times of Laminar Separated Flows," AIAA J., Vol. 9, No. 11, Nov., 1971.

FACILITY	M_∞	U_∞ (m/s)	Re_∞ (1/ft) *10-6	p_∞ (Pa)	T_∞ (˚K)	$P_{t,2}$ (kPa)	$T_{t,2}$ (˚K)	h_0-h_w (MJ/kg)
31 " Mach 10 Air	9.68	1413	0.506	70.11	53.0	8.52	1004	0.751
31 " Mach 10 Air	9.78	1452	0.967	130.1	52.5	16.22	1016	0.764
31 " Mach 10 Air	9.93	1434	1.897	242.3	51.2	31.02	1016	0.765
HYPULSE (CO_2)	9.74	4788	0.203	1182	1090	128.5	3693	12.35
HYPULSE (air)	7.86	5163	0.200	1842	1136	147.6	6037	14.18

TABLE 1 - Representative Operating Conditions of Test Facilities

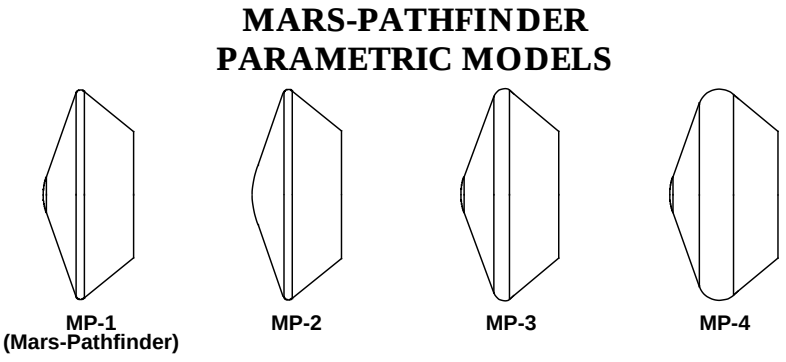

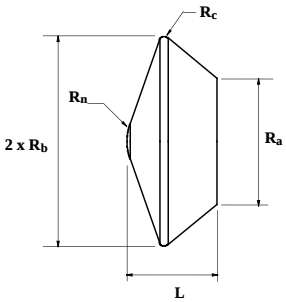

MODEL DIMENSIONS

MODEL	CONFIGURATION	R_n	R_b/R_n	R_a/R_n	R_n/R_c	L/R_n
MP-1	70˚ SPHERE-CONE	0.5"	2.0	1.2	10	1.723
MP-2	70˚ ASYMPTOTE HYPERBOLOID	0.5"	2.0	1.2	10	1.668
MP-3	70˚ SPHERE-CONE	0.5"	2.0	1.2	5	1.830
MP-4	70˚ SPHERE-CONE	0.5"	2.0	1.2	2.5	2.043

FIGURE 1 - Model Configurations and Dimensions

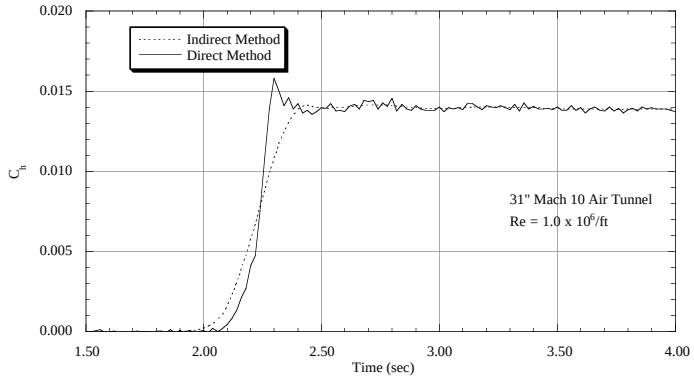

Figure 2. Direct and Indirect Method Heating Calculations for Stagnation Point Heating Time History

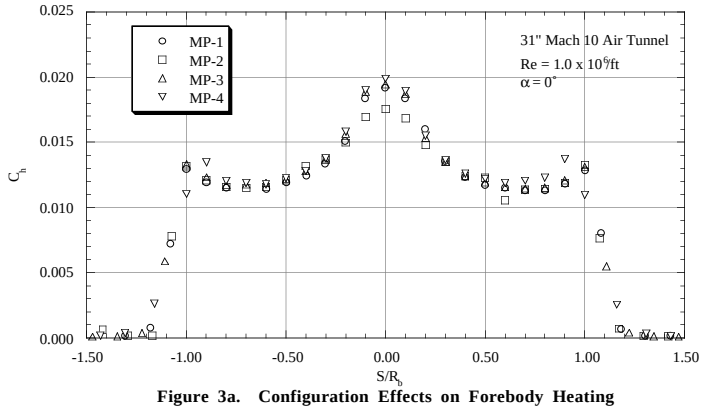

Figure 3a. Configuration Effects on Forebody Heating

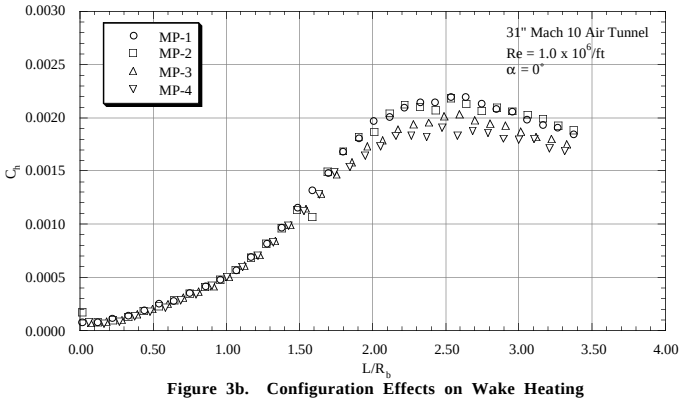

Figure 3b. Configuration Effects on Wake Heating

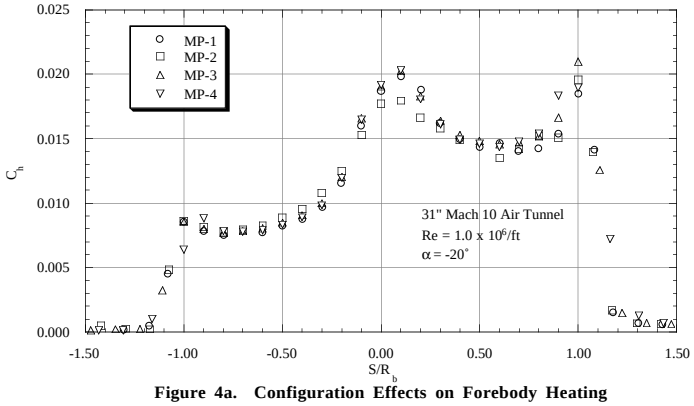

Figure 4a. Configuration Effects on Forebody Heating

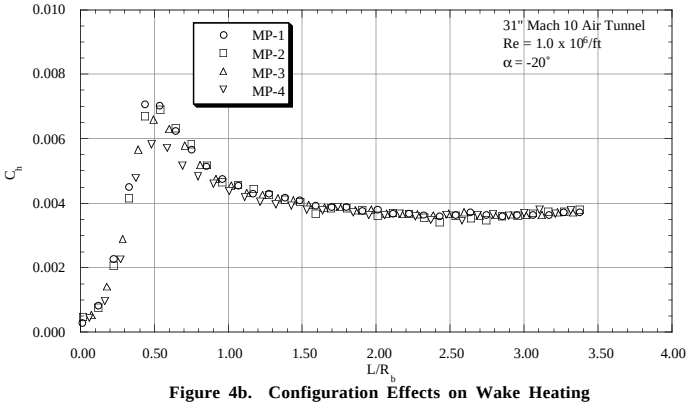

Figure 4b. Configuration Effects on Wake Heating

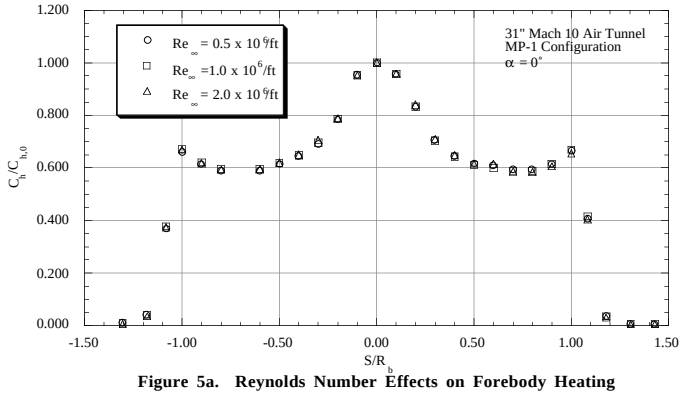

Figure 5a. Reynolds Number Effects on Forebody Heating

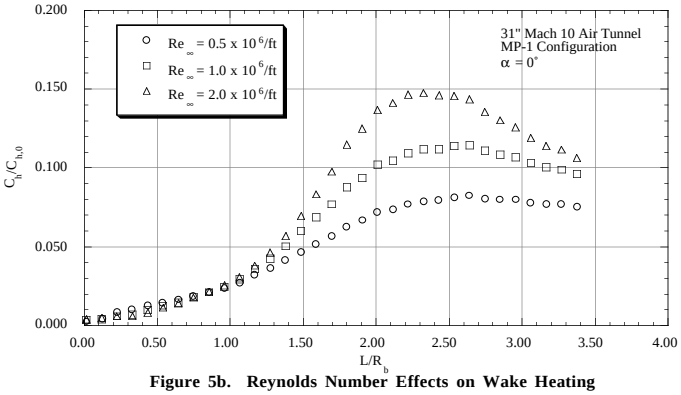

Figure 5b. Reynolds Number Effects on Wake Heating

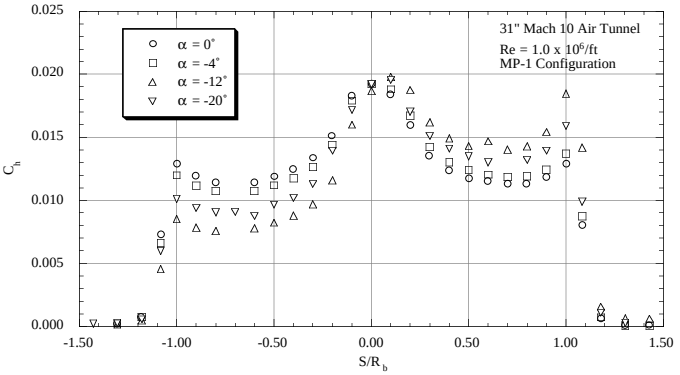

Figure 6a. Angle-of-Attack Effects on Forebody Heating

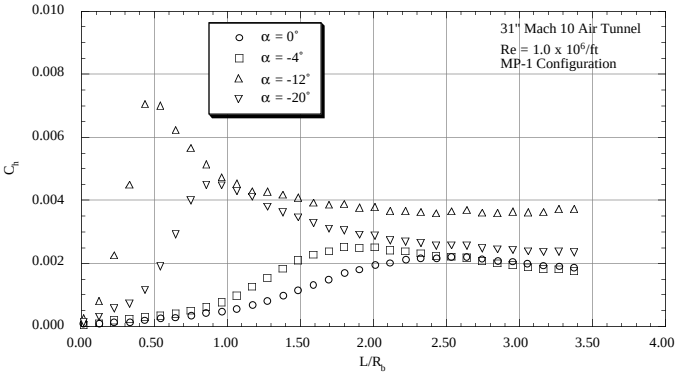

Figure 6b. Angle-of-Attack Effects on Wake Heating

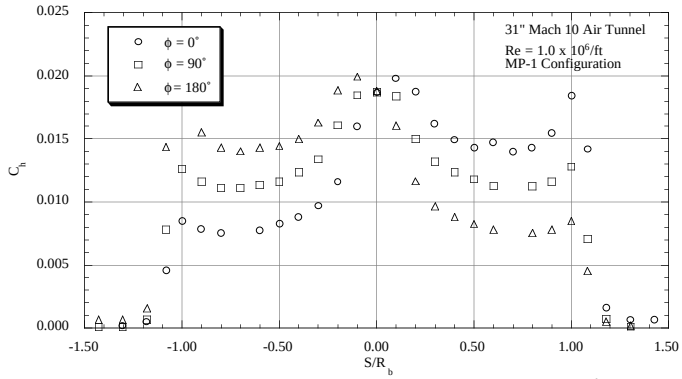

Figure 7a. Forebody Heating Distributions at α = -20˚

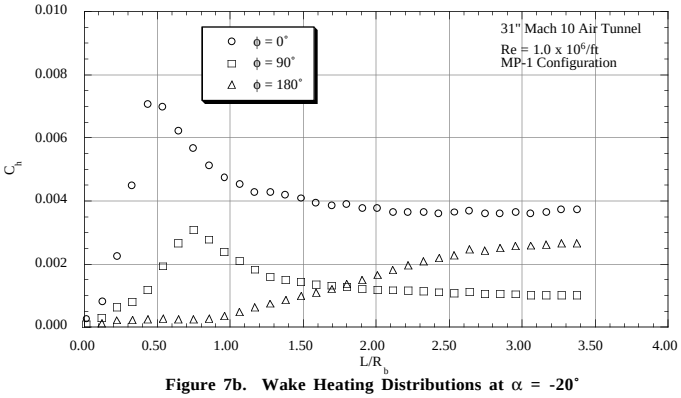

Figure 7b. Wake Heating Distributions at α = -20˚

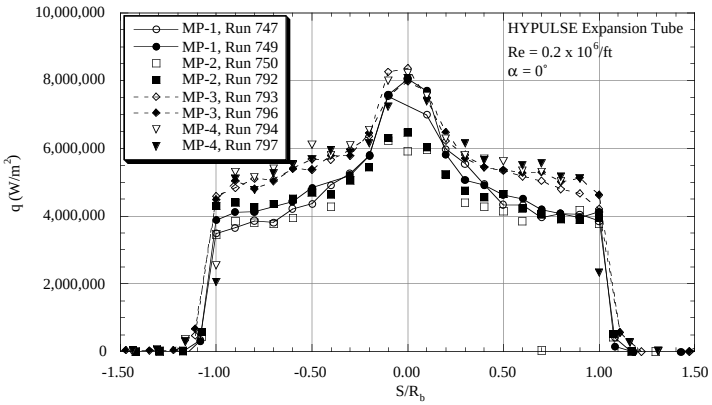

Figure 8. Configuration Effects on Forebody Heating, CO_2 Test Gas

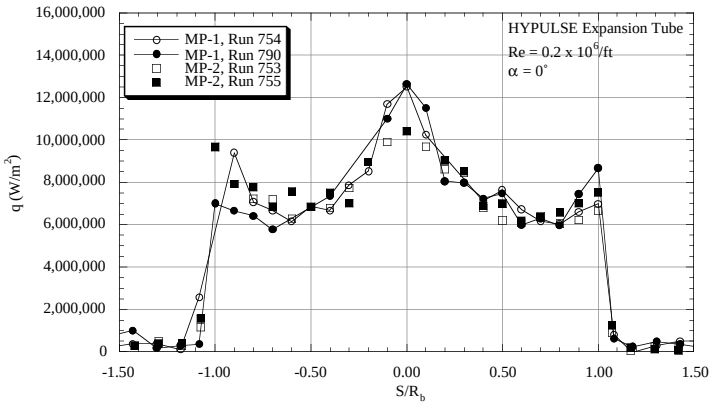

Figure 9. Configuration Effects on Forebody Heating, Air Test Gas

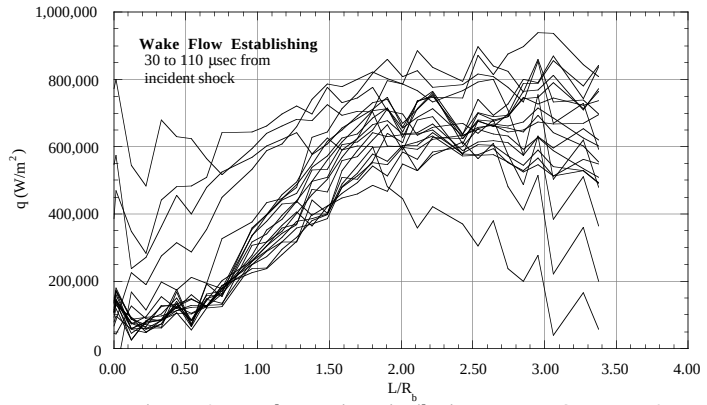

Figure 10a. Wake Heating Distributions, HYPULSE Run 749, MP-1 Configuration, CO_2 Test Gas

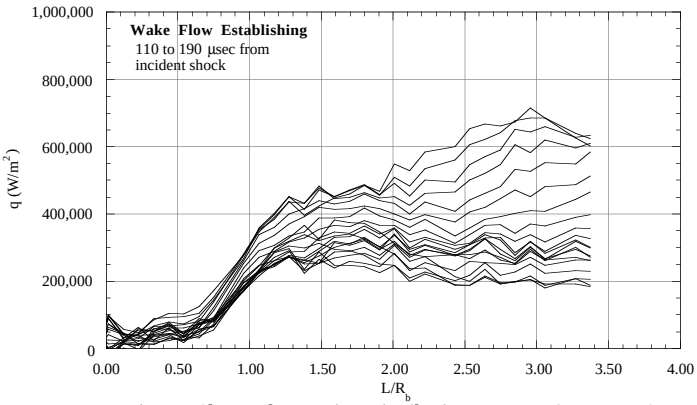

Figure 10b. Wake Heating Distributions, HYPULSE Run 749, MP-1 Configuration, CO_2 Test Gas

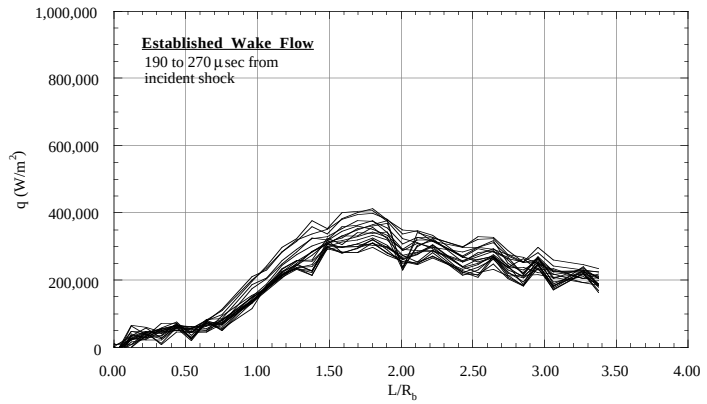

Figure 10c. Wake Heating Distributions, HYPULSE Run 749, MP-1 Configuration, CO_2 Test Gas

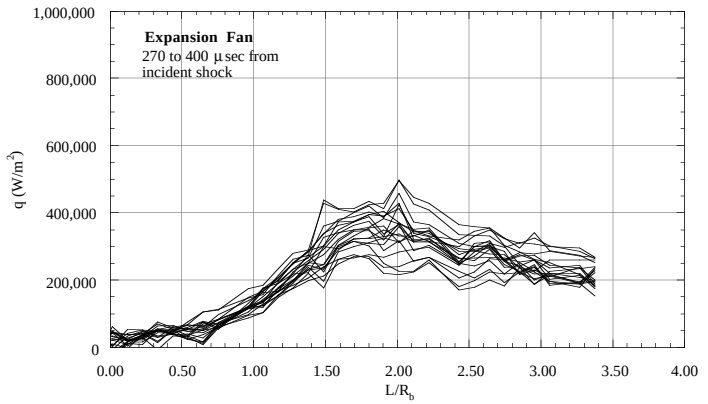

Figure 10d. Wake Heating Distributions, HYPULSE Run 749, MP-1 Configuration, CO_2 Test Gas

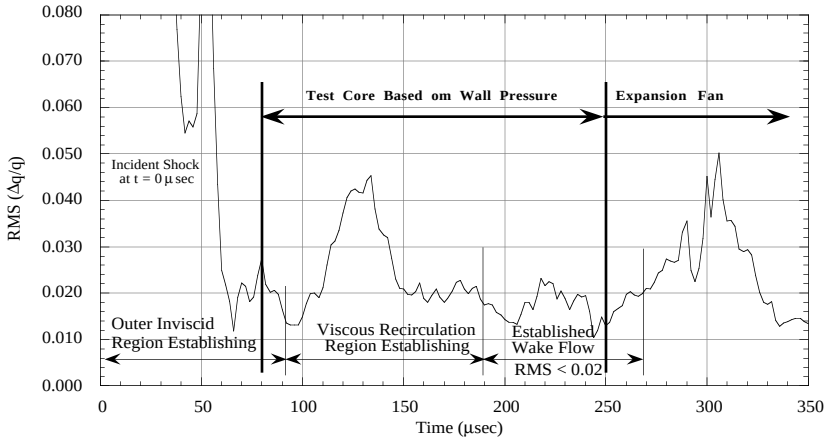

Figure 11. Wake Heating Residual, HYPULSE Run 749, MP-1 Configuration, CO_2 Test Gas

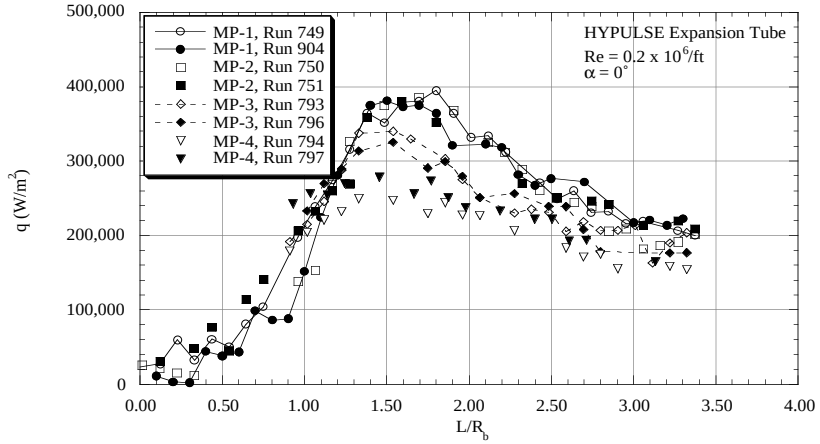

Figure 12. Configuration Effects on Wake Heating, CO_2 Test Gas

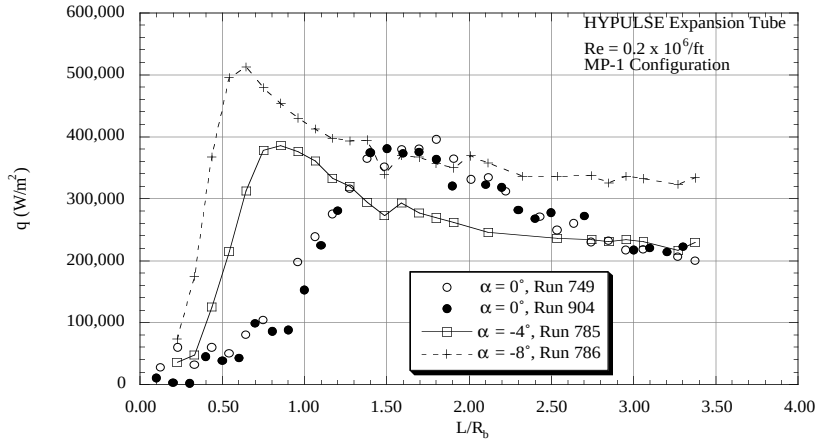

Figure 13. Angle-of-Attack Effects on Wake Heating, CO_2 Test Gas

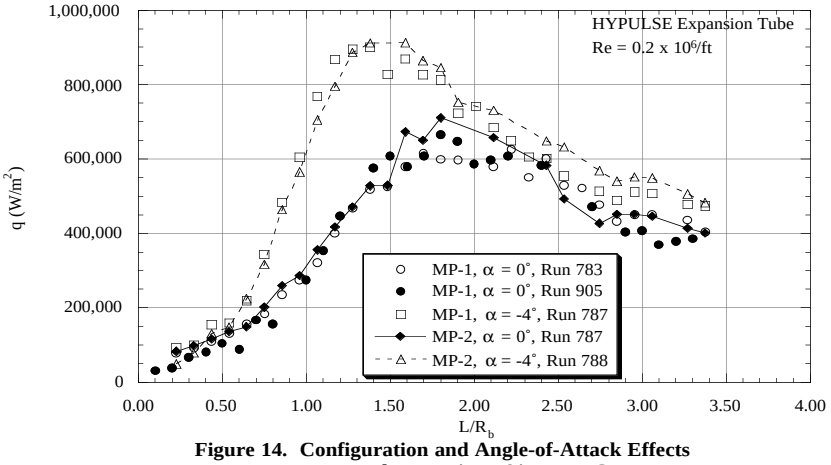

Figure 14. Configuration and Angle-of-Attack Effects on Wake Heating, Air Test Gas

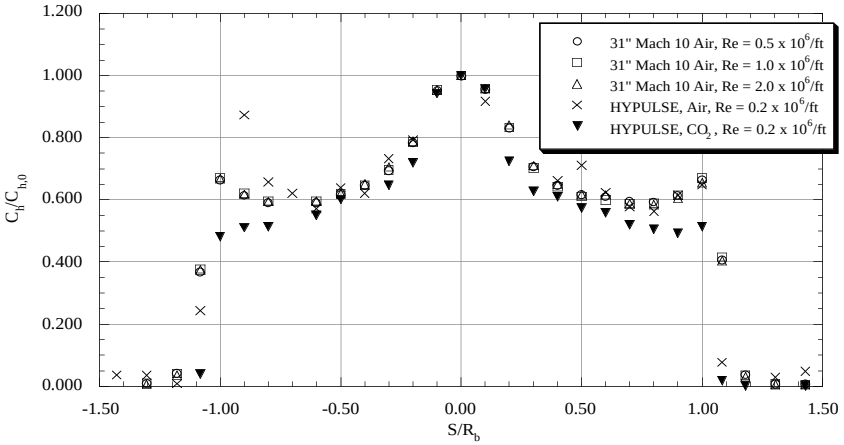

Figure 15. 31" Mach 10 and HYPULSE Normalized Forebody Heating Distributions, MP-1 Configuration

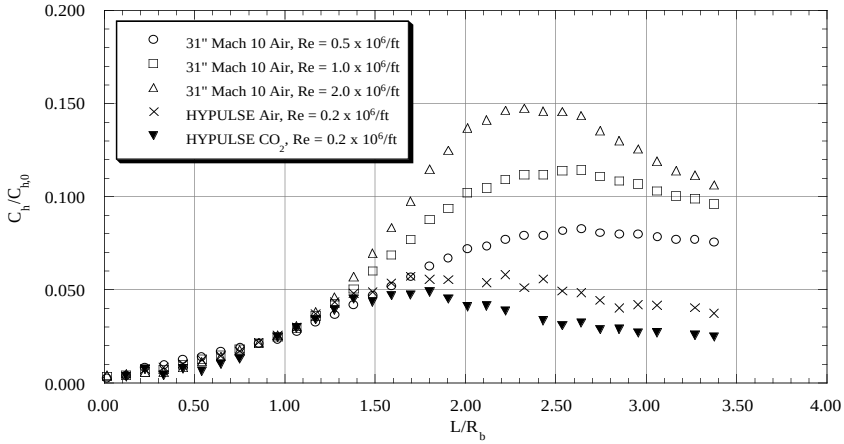

Figure 16. 31" Mach 10 and HYPULSE Normalized Wake Heating Distributions, MP-1 Configuration